Cell Prolif. 2007, **40**, 213–230

Amino-terminal deletion of heparin-binding epidermal growth factor-like growth factor$_{4–127}$ stimulates cell proliferation but lacks insulin-like activity

Z. Zhou and P. A. Harding

Department of Zoology, Miami University, Oxford, OH, USA

Received 3 *August* 2006*; revision accepted* 23 *November* 2006

Abstract. Heparin-binding epidermal growth factor-like growth factor (HB-EGF) Northern analysis demonstrated a novel 0.8-kb liver-specific HB-EGF transcript in addition to the endogenous 2.5-kb HB-EGF full-length transcript present in kidney, lung and liver tissues. Reverse transcriptase-polymerase chain reaction screening of liver RNA suggests that the 0.8-kb HB-EGF transcript lacks at least a portion of the amino-terminal EGF-like domain. In light of these data, we have constructed a human HB-EGF cDNA (HB-EGF$_{\Delta N}$) which lacks 373 bp, encoding the majority of the extracellular EGF-like domain, while maintaining the ectodomain 'shedding' site, transmembrane and cytoplasmic domains. *Objective*: The goal of this study is to characterize the ability of HB-EGF$_{\Delta N}$ to (i) stimulate cell proliferation and (ii) determine whether down-regulation of insulin-like growth factor-binding protein (IGFBP)-3 and -4 mRNA is regulated by soluble, mature HB-EGF or HB-EGF C. *Materials and methods*: HB-EGF$_{\Delta N}$ encodes nucleotides +1–10 of exon 1 linked to nucleotides 383–627 of the carboxy-terminal portion of exon 3 through exon 5. *Results*: Expression of HB-EGF$_{\Delta N}$ in mouse fibroblasts (MLC) resulted in 6.5- and 8-kDa HB-EGF immunoreactive proteins, stimulated tyrosine phosphorylation of p42 kDa and cell proliferation in MLC, but lacked the ability to bind EGF receptors. Finally, HB-EGF$_{\Delta N}$ failed to down-regulate IGFBP-3 and -4 mRNA when expressed in normal rat kidney cells. *Conclusions*: These findings demonstrate that amino-terminally truncated, membrane-bound form of HB-EGF stimulates cell proliferation but lacks insulin-like signalling, suggesting that insulin-like signalling is mediated by soluble, mature HB-EGF binding to EGF receptors.

INTRODUCTION

Heparin-binding epidermal growth factor-like growth factor (HB-EGF), originally identified in conditioned media from the human macrophage-like cell line, U-937 (Besner *et al.*

Grant Sponsor: Miami University Grant to Promote Research (to PAH)
Correspondence: Paul A. Harding, Department of Zoology, Miami University, Oxford, OH 45056, USA. Tel.: +1(513)5293187; Fax: +1(513)5296900; E-mail: hardinpa@muohio.edu

1990), is a member of the EGF superfamily, including transforming growth factor alpha (TGF-α) (Derynck *et al.* 1984), amphiregulin (AR) (Plowman *et al.* 1990), betacellulin (BTC) (Shing *et al.* 1997) vaccinia growth factor (VGF) (Stroobant *et al.* 1985) epiregulin (Toyoda *et al.* 1995) and the Neuregulin (NRG) family (Plowman *et al.* 1993). These EGF family members are initially synthesized as membrane-bound proteins that undergo extensive proteolytic processing (Massague & Pandiella 1993; Nanba *et al.* 2003). Most EGF-related proteins exhibit the ability to bind and stimulate autophosphorylation of the 170-kDa EGF receptor (EGFR), with the exception of NRG (Higashiyama *et al.* 1991, 1992; Carraway *et al.* 1997; Chang *et al.* 1997). The EGF-like domain of all family members encodes a conserved six-cysteine, 36–37 amino acid long motif that is collectively referred to as the EGF-like domain and appears to be essential in conferring the ability to bind EGFRs (Higashiyama *et al.* 1991).

Membrane-bound human HB-EGF (pro-HB-EGF) is composed of a signal peptide $\text{sequence}_{1–23}$, propeptide $\text{sequence}_{24–62}$, mature $\text{HB-EGF}_{63–149}$, $\text{juxtamembrane}_{150–160}$, $\text{transmembrane}_{161–184}$ and $\text{cytosolic}_{185–208}$ domains (Higashiyama *et al.* 1991, 1992). Membrane-bound pro-HB-EGF is biologically active in a non-diffusible juxtacrine manner capable of signalling neighbouring cells, possibly functioning as a negative regulator of cellular proliferation (Higashiyama *et al.* 1995; Nakamura *et al.* 2001). Pro-HB-EGF undergoes proteolytic processing by furin (Nakagawa *et al.* 1996) followed by ectodomain 'shedding' by a disintegrin and metalloprotease (ADAM) 9, 10, 12 or 17 (Izumi *et al.* 1998; Asakura *et al.* 2002; Lemjabbar & Basbaum 2002; Sunnarborg *et al.* 2002; Yan *et al.* 2002) resulting in the release of soluble, mature HB-EGF (Asakura *et al.* 2002). Ectodomain 'shedding' of pro-HB-EGF is induced by the phorbol ester 12-*O*-tetadecanoylphorbol-13-acetate (TPA) (Goishi *et al.* 1995). Subsequent and dependent on ectodomain 'shedding', the HB-EGF intracellular domain is processed by a yet unknown mechanism generating a carboxy-terminal HB-EGF domain, termed HB-EGF C (Nanba *et al.* 2003). Mature, soluble HB-EGF and HB-EGF C are each capable of stimulating cell division in EGFR-dependent and EGFR-independent manners, respectively (Nanba *et al.* 2003). However, the specific signalling pathways mediated by each HB-EGF domain upon processing are unknown.

Previous research has well documented mature, soluble HB-EGF stimulation of cell proliferation in a number of systems, by binding EGFRs (Raab & Klagsbrun 1997; Nishi & Klagsbrun 2004). HB-EGF C too stimulates cell proliferation by an EGFR-independent mechanism, but its signalling pathways have not been as well characterized. Recently, HB-EGF transgenic mice exhibited the ability to down-regulate insulin-like growth factor-binding protein (IGFBP)-3 and -4 mRNA in the kidney, suggestive of a possible role in insulin-like signalling (Provenzano *et al.* 2005). The six known IGFBPs are key regulatory molecules that bind insulin-like growth factor (IGF) I and II controlling their actions, such as cell population growth and differentiation (Rajaram *et al.* 1997; Hwa *et al.* 1999).

Because pro-HB-EGF is capable of cell signalling by at least two mechanisms, soluble, mature HB-EGF and HB-EGF C, these two domains must be separated in order to begin to discern their respective signalling pathways. Here, we have shown an amino-terminal truncated, membrane-bound HB-EGF protein that lacks a functional EGF-like domain (but maintains its HB-EGF C domain) undergoes proteolytic processing resulting in stimulation of cell division when stably expressed in MLCs. Additionally, this HB-EGF analogue fails to bind EGFRs on A431 cells and stimulates the insulin-like signalling pathway in normal rat kidney (NRK) cells, as compared to the full-length HB-EGF cDNA, suggesting that the insulin-like signalling pathway is mediated by soluble mature HB-EGF interacting with EGFRs.

MATERIALS AND METHODS

Northern blot analysis and reverse transcriptase-polymerase chain reaction

Total cellular RNA was extracted from kidney, lung and liver tissues (TriReagent, Molecular Research Center, Cincinnati, OH, USA), DNase-digested, and was quantified by absorbance at 260 nm according to manufacturer's recommendations.

For Northern blot analysis, RNA (10 μg) in glyoxal sample buffer (Cambrex, Rockland, ME, USA) was separated using 1% agarose in 1× MOPS buffer then transferred to immobilon membranes (Millipore Corp., Billerica, MA, USA) in 10× SSC for 16 h by capillary action. The blot was rinsed in 2× SSC at 68 °C (20 min) and was prehybridized in 5 ml of ExpressHyb (Clontech, Palo Alto, CA, USA) at 68 °C (30 min). A full-length 632-bp hHB-EGF cDNA was radiolabelled with α-^{32}P-dCTP using Ready-To-Go DNA Labelling Beads (dCTP) (Amersham Biosciences, Piscataway, NJ, USA) and was purified with a Probe Quant G-50 micro Spin column (Amersham Biosciences). The radiolabelled probe was heat denatured, placed in 5 ml of preheated ExpressHyb solution (68 °C), added to the membrane, and was incubated in a rotary oven at 68 °C (1 h). The hybridization solution was removed and the membrane was washed twice in 50 ml of 2× SSC/0.05% SDS at room temperature (30 min) with continuous agitation followed by a 30-min wash in 50 ml of 0.1× SSC/0.1% SDS at 50 °C (30 min). The membrane was wrapped in plastic wrap and was exposed to a phosphor storage screen for 16 h before imaging using the Storm 860 Phosphorimager (Molecular Dynamics, Piscataway, NJ, USA). Additionally, the blot was stripped and incubated with a radiolabelled DNA fragment encoding the L32 ribosomal subunit as an internal control to assure equivalent amounts of RNA from each tissue were analysed (Fig. 1a, bottom panel).

Total RNA (10 μg) was subjected to reverse transcriptase-polymerase chain reaction (RT-PCR) using a Superscript One-step RT-PCR kit (Invitrogen, Carlsbad, CA, USA) with an HB-EGF forward and reverse primer set: forward (5′-ACGTCGCGGATATCATGAAGCTGC-3′) and reverse (5′-ACGTGGCAGAATTCTCAGTGGG-3′) (Fig. 1b, pane 1). RT-PCR using RNA isolated from pMT-HB-EGF, pMT-HB-EGF$_{\Delta N}$ and pSV-neo^{r} mouse fibroblast stable cell lines was performed using an exon 4 forward primer (5′-CTCCCAGTGGAAAATCGC-3′) and the above the HB-EGF reverse primer (Fig. 1b, panel 2) and an exon 4 reverse primer (5′-GCGATTTCCACTGGGAG-3′) and the HB-EGF forward primer (Fig. 1b, panel 3). A glycecaldehyde phosphate dehydrogenase (GAPDH) forward primer (5′-CTACACTGAGGACCAGGTTGTC-3′) plus a GAPDH reverse primer (5′-GCCTCTCCTGCTCAGTGTCCTTGC-3′) was used as an internal control to assure integrity of the RNA samples (Fig. 1b, panel 4). RT-PCR was performed using the following parameters: one cycle of 53 °C (30 min) followed by 30 cycles of 94 °C (30 s), 54 °C (1 min), 72 °C (45 s), followed by an extension at 72 °C (15 min). The PCR products were analysed by agarose gel electrophoresis and were stained with ethidium bromide.

DNA sequencing, cloning and stable expression

A 250-bp human HB-EGF cDNA encoding nucleotides 383–627 of exon 3 through exon 5 including the translational stop codon was amplified by PCR, purified (Qiagen, Valencia, CA, USA), sequenced and cloned downstream of +1–10 of exon 1 of HB-EGF and termed HB-EGF$_{\Delta N}$. HB-EGF$_{\Delta N}$ expression is controlled by the mouse metallothionein promoter-1 (MT-1) (Harding *et al.* 1999). The full-length 627-bp human HB-EGF cDNA has previously been cloned into the MT-1 expression vector, pMT-1: HB-EGF (Harding *et al.* 1999).

Cell culture and transfection

MLC and NRK cells were maintained in Dulbecco's minimal essential medium (DMEM) (Cellgro, Herndon, VA, USA) supplemented with 10% foetal bovine serum, penicillin (100 U/ml) and

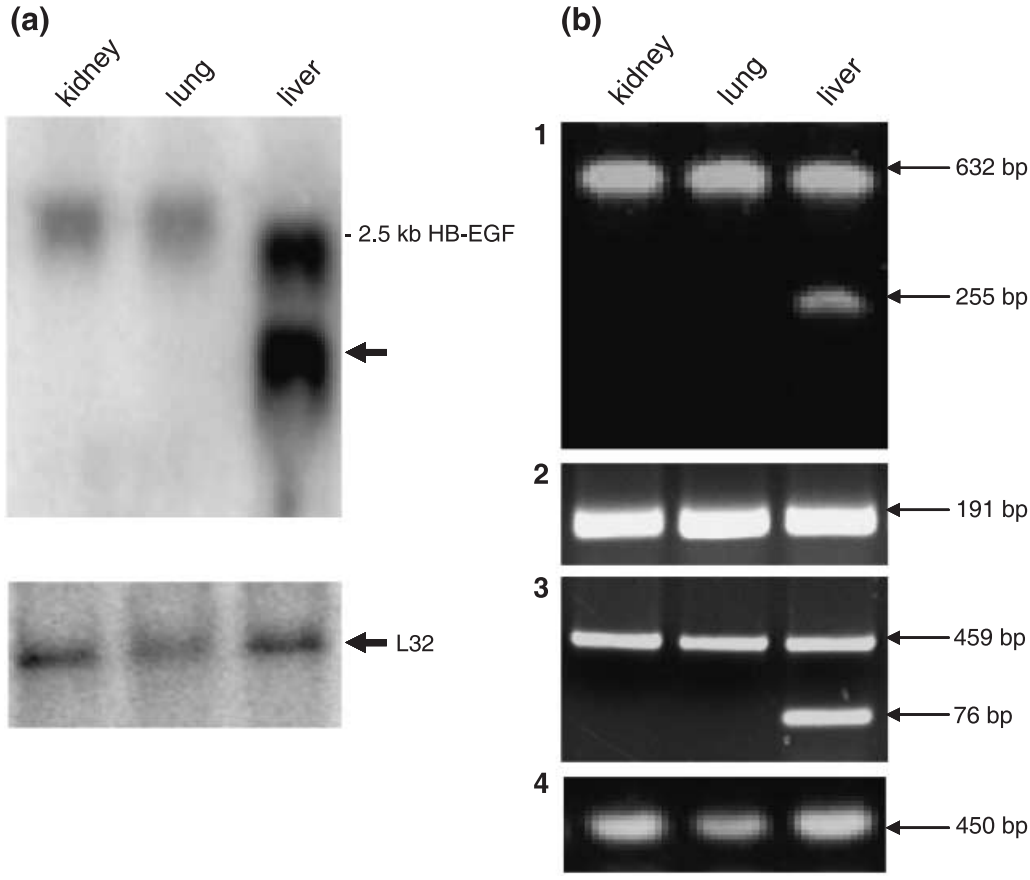

Figure 1. RNA analyses from FVB/N mouse tissues. (a) Northern blot analysis of total RNA (10 μg) from kidney, lung and liver tissue, probed with a radiolabelled HB-EGF cDNA. The full-length 2.5-kbp HB-EGF transcript is observed in all tissues. A shorter HB-EGF transcript (~1 kb) is present only in liver tissue, as indicated with the arrow (a, top panel). A ^{32}P-labelled L32 ribosomal subunit was used to assure equivalent amounts of RNA were analysed (a, bottom panel). (b) Semi-quantitative RT-PCR of 1 μg of total cellular RNA from kidney, lung and liver tissues resulted in the predicted full-length 632-bp mouse HB-EGF cDNA in all tissues and a 255-bp RT-PCR product is present only in liver tissue (b, panel 1). Primer sets used to amplify a short segment of the extracellular domain, transmembrane domain and complete intracellular domain and the amino-terminus to exon 4 was amplified to determine possible alternative splicing within the intracellular- and extracellular-encoded regions of the HB-EGF transcript, respectively. A single 191-bp product was observed in all tissues using the primer set to amplify exon 4 – stop, suggestive of alternative splicing occurring in the amino-terminus (b, panel 2). A single 459-bp product was observed in all tissues using the primer set to amplify the start – exon 4 while a 76-bp product was only observed in liver (b, panel 3). GAPDH primers were used as an internal control (450 bp), as indicated (b, panel 4).

streptomycin (100 μg/ml) (BioWhitaker, Walkersville, MD, USA). Either pMT-HB-EGF or pMT-HB-EGF$_{\Delta N}$ (4.0 μg each) and 400 ng pSV-neo were cotransfected into MLC or NRK cells using Lipofectamine (Invitrogen) according to the manufacturer's recommendations. pSV-neo alone was transfected into each cell type for a control cell line. Forty-eight hours post-transfection, the cells were placed on neomycin (G418) selection (1 mg/ml). Single colonies were picked and propagated generating neomycin resistant pMT-HB-EGF, pMT-HB-EGF$_{\Delta N}$ and pSV-neo stable cell lines.

Affinity purification of HB-EGF C antibody

Polyclonal antiserum against human HB-EGF C was generated using a synthetic 16 amino acid peptide corresponding to amino acids 193–208 of the deduced human HB-EGF amino acid sequence. The peptide sequence (NH_2-DVENEEKVKLGMTNSH-COOH) was sent to Zymed Laboratories, Inc. (San Francisco, CA, USA) where it was synthesized and conjugated to Keyhole Limpet Hemocyanin and was used to immunize two rabbits in order to produce anti-human HB-EGF C polyclonal antibody. Sera from the injected rabbits were affinity-purified using a SulfoLink Kit column (Pierce Biotechnology, Inc., Rockford, IL, USA) containing a 6% cross-linked agarose support conjugated to the peptide used in the immunization. The concentration of purified HB-EGF C antibody was quantified spectrophotometrically at 280 nm.

Western blot analysis

Cell extracts from pMT-HB-EGF$_{\Delta N}$, pMT-HB-EGF and pSV-neo stable cell lines were collected by scraping the cell monolayer in phosphate-buffered saline (PBS)/1% 3-[3-(cholomidopropyl) dimethylammonio]-1-propane sulfonate, homogenized, centrifuged at 13.4 ***g*** for 15 min at 4 °C, and was quantified using a bicinchoninic acid (BCA) protein assay kit (Pierce Biotechnology, Inc.). Additionally, membrane preparations were obtained from two 160 mm^2 dishes of pMT-HB-EGF$_{\Delta N}$ MLC stable cell line as described (Jewell & Lingrel 1991) omitting the NaI step and quantified using a BCA protein assay kit (Pierce Biotechnology, Inc.). 15 μg of total protein was suspended in 2× sample buffer, separated by 12.5% SDS-PAGE and was electrophoretically transferred to immobilon P^{SQ} nylon membranes (Millipore Corp.) in 25 mM Tris-HCl, 192 mM glycine (TBS), 10% methanol overnight at 25 V at 4 °C. Membranes were blocked for 1 h in TBS/3% bovine serum albumin (BSA) then were incubated with an anti-HB-EGF-C peptide antisera (2 μg/ml) with constant agitation for 2 h at room temperature, rinsed three times for 5 min each in TBS, and then were incubated with horseradish peroxidase (HRP)-conjugated mouse anti-rabbit immunoglobulin G antibody (1 : 5000) (Jackson ImmunoResearch Laboratories, West Grove, PA, USA). Specific immunoreactivity was determined by application of SuperSignal West Pico Chemiluminescent Substrate (Pierce Biotechnology, Inc.) to the membrane. Immunoblots were stripped and incubated with a mouse actin antibody (1 : 70 000) overnight at 4 °C, washed and incubated with goat antimouse HRP-conjugated immunoglobulin G antibody (1 : 80 000), and developed as described above. Specificity of HB-EGF antisera was demonstrated by HB-EGF immunoblots incubated with antisera (0.5 μg/ml) along with excess peptide resulting in loss of immunoreactive HB-EGF proteins (data not shown).

Tyrosine phosphorylation in response to HB-EGF or HB-EGF$_{\Delta N}$

Cell lysates (15 μg) from each of HB-EGF, HB-EGF$_{\Delta N}$ and pSV-neo^r stably transfected MLC were obtained by scraping cells in lysis solution (1% Triton-X100, 100 mM Tris pH 7.4), they were quantified, and analysed by Western blot analysis as described above. In order to discern possible differences in HB-EGF and HB-EGF$_{\Delta N}$ signalling through tyrosine phosphorylation pathways, membranes with lysates from each stable cell line were incubated with mouse anti-phosphotyrosine-HRP antibody, 1 : 2000 (Zymed Laboratories) 2 h at room temperature with gentle agitation, washed 3 × 5 min each in TBS, and immunoreactive tyrosine phosphorylated proteins were determined by application of SuperSignal West Pico Chemiluminescent Substrate (Pierce Biotechnology, Inc.) and developed.

Competitive binding assay

To address whether proteins derived from proHB-EGF, HB-EGF$_{\Delta N}$ and pSV-neo MLC stable cell lines are able to bind EGFRs, competitive EGF radioreceptor assays were performed using

^{125}I-EGF (PerkinElmer, Boston, MA, USA) and human squamous epidermoid carcinoma cells (A431). A431 cells were maintained in DMEM containing 10% FBS and 50 μg/ml penicillin/streptomycin, plated at a density of 2×10^4 cells/well/0.5 ml in 48-well plates and propagated overnight. Following overnight growth, media were removed and replaced with DMEM minus serum. The cells were then allowed to equilibrate for 2 h. Medium was removed and the cell monolayer was washed with 250 μl cold binding medium (DMEM containing 0.1% BSA, pH 7.2). After this incubation, the cells were placed at 4 °C for 1.5 h to equilibrate. ^{125}I-EGF (2.5 ng/ml) in 150 μl of cold binding medium was added to each well along with increasing amounts of lysates from pro-HB-EGF, HB-EGF$_{\Delta N}$ or pSV-neo stable cell lines in serial dilution from 10^{-3} to 100 μl of total cell lysate. Equivalent amounts of HB-EGF from the cell lysates were quantified by Western blot to determine relative concentration thus equivalent amounts of HB-EGF were added to each well. Equivalent volumes of lysate from pSV-neo stably transfected MLC were assayed as a control to assure no EGFR ligand was present in MLC that competed with ^{125}I-EGF binding to A431 cells. A recombinant HB-EGF standard (R&D Systems) was assayed in increments ranging from 0.01 ng to 200 ng. Lysates of pro-HB-EGF and analogues were tested for their ability to displace ^{125}I-EGF in the radioreceptor assays. To accomplish this, lysates were harvested by scraping the cells from the plates and subjecting them to sonification. A431 cells were incubated under the above conditions at 4 °C for 2 h, washed three times with cold PBS and were solublized in 250 μl of 0.3 N NaOH (two collections) and counted in a γ-counter. Two binding assays performed in triplicate ± SEM are indicated for each stable cell line.

Cell growth curve analyses

Selected pMT-HB-EGF$_{\Delta N}$, pMT-HB-EGF and pSV-neo stable cell lines (2 each) were plated at a density of 2×10^4 cells in 60 mm^2 culture dishes in DMEM containing 10% FBS in triplicate. Cells were trypsinized in 0.5 ml and were collected; each well was washed with 0.5 ml PBS, and combined. Cell number was determined every 24 h for 72 h using a haemocytometer. Additionally, cell growth rates were analysed in the presence of 10 μM PD98059, an inhibitor of extracellular signal-regulated kinase (ERK) phosphorylation known to inhibit ectodomain shedding of HB-EGF (Gechtman *et al.* 1999). The mean ± SEM of two experiments performed in triplicate was plotted. Statistical significance between each cell line was analysed using a two-way statistical analysis of variance (ANOVA). Values of $P = 0.05$ were considered to be significant.

IGFBP-3 and -4 mRNA analyses

In these experiments, pMT-HB-EGF$_{\Delta N}$, pMT-HB-EGF and pSV-neo NRK cells (2.0×10^5) were cultured in DMEM containing 10% FBS + penicillin/streptomycin (100 U/ml) in 60 mm dishes and were grown overnight. The following day, NRK cells were depleted of serum for 2 h followed by addition of 1 ml PBS containing HB-EGF (50 ng/ml) and incubated for 30 min (37 °C). Total cell RNA was isolated using TriReagent (Molecular Research Center, Cincinnati, OH, USA), quantified by absorbance 260, DNase treated (DNA Free, Ambion, Austin, TX, USA) and subjected to semi-quantitative RT-PCR using Superscript One-step RT-PCR kit (Invitrogen) using IGFBP primers listed in Table 1.

RESULTS

Characterization of an HB-EGF alternative transcript

Northern blot analysis was performed using cellular RNA from 7 week FVB/N mice to characterize HB-EGF mRNAs in kidney, lung and liver. The expected 2.5-kb full-length HB-EGF

Table 1. IGFBP-3–5 and GAPDH primer sets for semiquantitative RT-PCR

Primer	Size	Sense	Anti-sense
IGFBP-3	200 bp	AGTGAGTCCGAGGAGGACC	GACTCAGAGGAGAGTTCTGGG
IGFBP-4	513 bp	CTGCGGTTGTTGTGCCACTTGC	CAGCATTTGCCACGCTGTCCATC
IGFBP-5	484 bp	GCAGGACGAGGAGAAGCCGC	TCCACGCACCAGCAGATGCC
GAPDH	450 bp	CTACACTGAGGACCAGGTTGTC	GCCTCTCCTGCTCAGTGTCCTTGC

transcript was present in all tissues examined as well as a smaller ~0.8-kb transcript present only in liver (Fig. 1a, top panel). The level of HB-EGF full-length transcript was comparable to the smaller truncated HB-EGF transcript found in liver. Additionally, a ^{32}P-labelled L32 ribosomal subunit DNA fragment was used as an internal control to assure equal amounts of RNA from each tissue were analysed (Fig. 1a, bottom panel).

Semiquantitative RT-PCR results using these RNAs and a primer pair that immediately flank the coding translational start and stop codons of mHB-EGF resulted in full-length 632-bp HB-EGF cDNA in all tissues along with a shorter RT-PCR product, approximately 255 bp present only in the liver (Fig. 1b, panel 1). A single 191-bp product was observed in all three tissues when using a primer set designed to amplify the juxtamembrane, transmembrane and intracellular coding domains of HB-EGF, indicating that the truncation must lie upstream of the juxtamembrane coding region, which is consistent with the results in Fig. 1(b), panel 2. If the deletion had occurred within the intracellular coding region, a smaller RT-PCR product would have been detected. To demonstrate that the deletion occurred in the HB-EGF extracellular domain, the 5′ end of the HB-EGF transcript to exon 4 was analysed by RT-PCR resulting in a predicted 459-bp DNA product present in kidney, lung and liver tissues. Additionally, a smaller 76-bp RT-PCR product was identified in liver only (Fig. 1b, panel 3). This suggests that the deletion within the liver HB-EGF transcript occurred upstream of exon 4. GAPDH primers resulted in an expected 450-bp DNA product in all RNA samples (Fig. 1b, panel 4), indicating that equivalent amounts of RNA were analysed from each tissue. In light of these results, we have cloned and sequenced an equivalent 255-bp human HB-EGF cDNA encoding nucleotides +1–10 of exon 1 linked to nucleotides 383–627 of the carboxy terminal portion of exon 3 through exon 5. This clone, termed HB-EGF$_{\Delta N}$, encodes the translational start codon, a nonfunctional soluble HB-EGF domain (incapable of binding and activating EGFRs), Leu$_{148}$ (the cleavage site recognized by ADAMs), transmembrane domain and intracellular domain. This HB-EGF amino-terminal analogue is significant in that it appears *in vivo* suggesting that it may provide an important physiological role in the liver. The predicted HB-EGF$_{\Delta N}$ amino acid sequence encoding only a portion of the EGF-like domain including the third disulphide bond, juxtamembrane, transmembrane and cytoplasmic domains is outlined in Fig. 2(a). A comparison between the pro-HB-EGF and HB-EGF$_{\Delta N}$ protein structures is depicted in Fig. 2(b).

Expression of HB-EGF$_{\Delta N}$ in mammalian cells

To specifically determine whether the 255-bp HB-EGF$_{\Delta N}$ encodes biologically active protein, stable cell lines were established that each express pMT-HB-EGF$_{\Delta N}$, pMT-HB-EGF or pSV-neo using MLCs. MLCs were chosen because of lack of detectable HB-EGF expression, but are biologically responsive to HB-EGF, as described. Western blot analyses of membrane proteins and cell lysates derived from each stable cell line was performed using a peptide antibody directed against the C-terminus of HB-EGF in which two immunoreactive membrane-bound proteins of

(a)

```
***
ATGAAGCTGCGAGCTCCCTCCTGCATCTGCCGCCCGGGTTACCATGGAGAGAGGTGTCAT          60
M  K  L  R  A  P  S  C  I  C  R  P  G  Y  H  G  E  R  C  H           20

GGGCTGAGCCTCCCAGTGGAAAATCGCTTATATACCTATGACCACACAACCATCCTGGCC         120
G  L  S  L  P  V  E  N  R  L  Y  T  Y  D  H  T  T  I  L  A           40

GTGGTGGCTGTGGTGCTGTCATCTGTCTGTCTGCTGGTCATCGTGGGGCTTCTCATGTTT        180
V  V  A  V  V  L  S  S  V  C  L  L  V  I  V  G  L  L  M  F           60

AGGTACCATAGGAGAGGAGGTTATGATGTGGAAAATGAAGAGAAAGTGAAGTTGGGCATG        240
R  Y  H  R  R  G  G  Y  D  V  E  N  E  E  K  V  K  L  G  M           80

ACTAATTCCCACTGA                                                      255
T  N  S  H  ***                                                      85
```

(b)

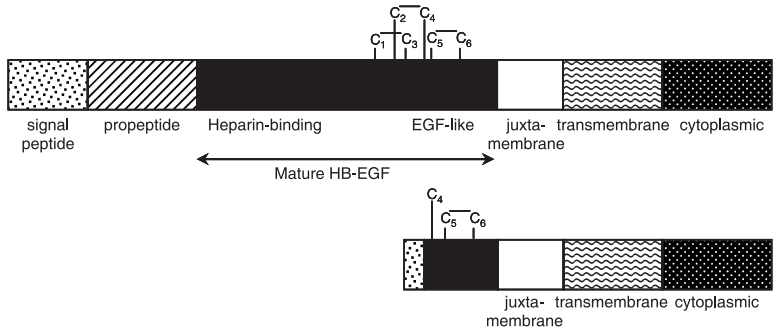

Figure 2. Nucleotide and primary translation product of human HB-EGF$_{\Delta N}$ cDNA. (a) Nucleotides and amino acids are numbered to the right of each line. Standard one-letter abbreviations are used to represent the amino acid residues. The first 10 nucleotides encode the first three amino acids of the signal peptide fused to exon 3 (boxed). The start and stop codons are indicated by asterisks. Underlined amino acids indicate the transmembrane domain. (b) Schematic representation of membrane bound pro-HB-EGF and HB-EGF$_{\Delta N}$ proteins.

6.5 kDa and 8 kDa, whereas only a 6.5-kDa protein was observed from the cell lysate (Fig. 3a, lanes 1 and 2, respectively). The 6.5-kDa and 8-kDa proteins are the proteolytically processed cytoplasmic domain (HB-EGF C) and membrane-bound forms of pMT-HB-EGF$_{\Delta N}$, respectively. Additionally, cell lysates from MLCs stably transfected with the full-length HB-EGF cDNA (pMT-HB-EGF), resulted in the presence of three HB-EGF immunoreactive proteins of 6.5 kDa, 20 kDa and 22 kDa (Fig. 3a, lane 4). The 6.5-kDa immunoreactive protein from lysates of pMT-HB-EGF is the same HB-EGF proteolytically processed cytoplasmic domain (HB-EGF C) identified from pMT-HB-EGF$_{\Delta N}$, cells. The 20-kDa and 22-kDa HB-EGF immunoreactive proteins obtained from lysates of pMT-HB-EGF are consistent with the two membrane-bound forms previously reported and exhibit amino-terminal heterogeneity due to proteolytic processing (Harding *et al.* 1999). As a control for specificity, no HB-EGF immunoreactive proteins were observed in cell lysates from pSV-neo stably transfected MLCs (Fig. 3a, lanes 3 and 5). It is noteworthy that the 8-kDa membrane-bound HB-EGF$_{\Delta N}$ protein is detected only in membrane preparations and not in the cell lysates, unlike the presence of the membrane-bound 20-kDa and 22-kDa proteins from pro-HB-EGF. This may suggest that HB-EGF$_{\Delta N}$ protein is either less abundant or more efficiently processed.

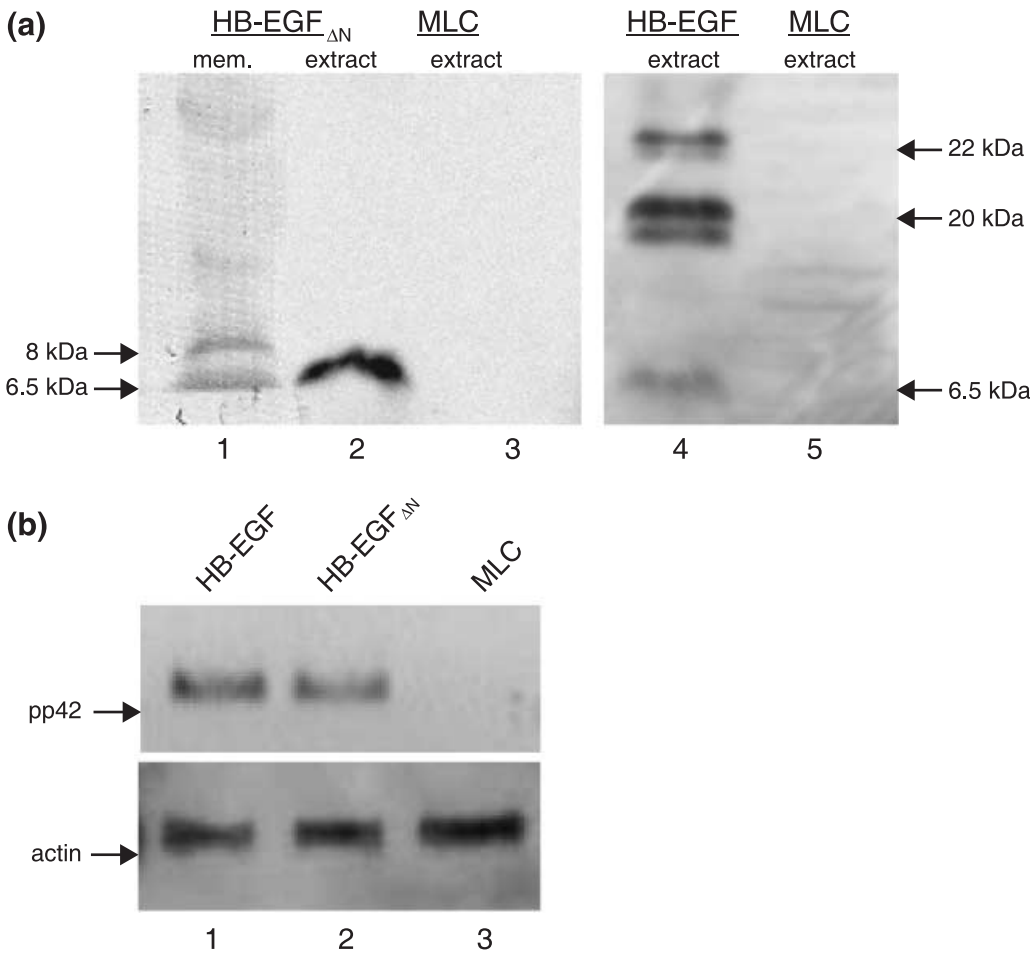

Figure 3. Identification of pro-HB-EGF and HB-EGF$_{\Delta N}$ ectodomain shedding. (a) Characterization of immunoreactive HB-EGF proteins from purified membrane preparations (lane 1) and cell extracts (lane 2) from pMT-1: HB-EGF$_{\Delta N}$ stably transfected cells. HB-EGF immunoreactive proteins from cell extracts from pMT-1: HB-EGF stable cell lines (lane 4). Cell extracts from neo^r MLC were used to demonstrate specific immunoreactive HB-EGF proteins (lanes 3 and 5). A 6.5-kDa protein (HB-EGF C) was observed in both HB-EGF$_{\Delta N}$ and HB-EGF stable cell lines. (b) Induction of tyrosine phosphorylated p42 (pp42) was observed from lysates of pMT-1: HB-EGF and pMT-1 HB-EGF$_{\Delta N}$ stable cell lines (Upper panel, lanes 1 and 2, respectively). No pp42 was observed in pSV-neo^r MLC (upper panel, lane 3). The membrane in the upper panel was stripped and incubated with a mouse actin antibody, resulting in 43 kDa immunoreactive proteins in all cell lysates (lower panel).

Stimulation of pp42

It is well established that protein tyrosine phosphorylation may play an integral role in the regulation of ectodomain shedding (Gechtman *et al.* 1999). To provide further evidence that specific proteolytic processing of HB-EGF$_{\Delta N}$ occurs in the pMT-HB-EGF$_{\Delta N}$ stable cell line, lysates from both pMT-HB-EGF$_{\Delta N}$ and pro-HB-EGF stable cell lines were examined using an anti-phosphotyrosine antibody. Lysates from these cells induced tyrosine phosphorylation of a 42-kDa protein, pp42 in stable MLCs that express the full-length pro-HB-EGF and HB-EGF$_{\Delta N}$ (Fig. 3b, lanes 1 and 2, respectively). No pp42 induction was observed in pSV-neo^r only MLCs (Fig. 3b, lane 3).

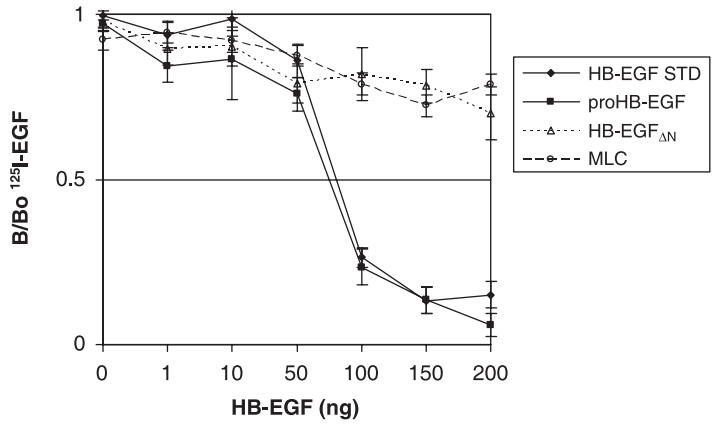

Figure 4. Competitive EGFR binding Assay. The ^{125}I-EGF bound versus unbound ratio is plotted in the presence of increasing amounts of unlabelled recombinant HB-EGF, pro-HB-EGF and HB-EGF$_{\Delta N}$. Lysates from MLC were used as a control. Each point represents the mean ± SEM for two experiments (each in triplicate).

Competitive EGFR binding assay

Proteins from pro-HB-EGF, HB-EGF$_{\Delta N}$ and pSV-Neo stable MLCs were examined for their ability to bind EGFRs along with recombinant mature HB-EGF (R&D Systems) that is known to bind EGFR. Lysates from each stable cell line were assayed for their ability to compete with ^{125}I-EGF in a competitive receptor binding assay using A431 epidermoid carcinoma cells that express approximately 2×10^6 million EGFRs per cell. Results indicate that recombinant HB-EGF and pro-HB-EGF displaced ^{125}I-EGF with similar effective concentrations to displace 50% of the ^{125}I-EGF (EC50) of approximately 75–80 ng, although lysates from pSV-neo MLC and HB-EGF$_{\Delta N}$ failed to displace ^{125}I-EGF (Fig. 4). In sum, these results suggest that HB-EGF$_{\Delta N}$, which lacks amino acids 4–127 encoding a partial signal peptide, pro-peptide, heparin-binding and a large part of the EGF-like domains, is not capable of binding EGFRs.

Cell growth curves

Stable expression of HB-EGF$_{\Delta N}$ in MLCs demonstrated proteolytic processing of HB-EGF, tyrosine phosphorylation of pp42 and the subsequent generation of 6.5-kDa HB-EGF C. In order to demonstrate that HB-EGF$_{\Delta N}$ is capable of stimulating cellular division in MLCs, the cell population growth rates of two independent cell lines each were determined at 24, 48 and 72 h, and compared to the growth rates of non-HB-EGF expressing cells (pSV-neo) and pro-HB-EGF stably transfected MLCs. First, HB-EGF and HB-EGF$_{\Delta N}$ stable cell lines that express similar levels of HB-EGF mRNA were chosen for determination of growth rates. Expression of HB-EGF mRNA was determined by semiquantitative RT-PCR using primers that recognize the HB-EGF mRNA encoding the juxtamembrane domain of HB-EGF and the C-terminus of HB-EGF. Similar levels of the predicted 191-bp DNA product was observed in HB-EGF, and HB-EGF$_{\Delta N}$ stable cells, while no 191-bp DNA product was observed in the pSV-neo^r control cell line (Fig. 5a, top panel). As an internal standard, RT-PCR using GAPDH primers resulted in an expected 450-bp DNA product in all RNA samples (Fig. 5a, bottom panel).

Next, HB-EGF growth curves using these cell lines were generated by counting the total number of cells every 24 h for a 72-h period. Significant differences in growth rates were observed with MLC that stably express HB-EGF$_{\Delta N}$ or pro-HB-EGF as compared to pSV-neo^r MLCs at 48 and 72 h. HB-EGF$_{\Delta N}$ and pro-HB-EGF stable cell lines grew at accelerated rates on average of 1.34× and 1.72× at 48 h and 1.56× and 2.04× at 72 h, respectively, as compared to pSV-neo^r MLCs. The average cell number of two experiments performed in triplicate were plotted to generate the growth curves for pro-HB-EGF, HB-EGF$_{\Delta N}$ and pSV-neo^r MLCs and are shown in Fig. 5(b) and are representative of each of two pro-HB-EGF, HB-EGF$_{\Delta N}$ and pSV-neo^r stable cell lines examined. The standard error for each time point for each cell type is indicated.

In order to eliminate the effects of processed forms of HB-EGF (soluble, mature HB-EGF and HB-EGF C) on stimulation of cell proliferation, the rates of cell division were analysed every 24 h over a 72-h period in the presence of 10 μm PD98059, an inhibitor of mitogen activated protein (MAP) kinase kinase (also known as MEK) phosphorylation. MAP kinase activation (pp42) is required for HB-EGF proteolytic processing (Gechtman *et al.* 1999; Umata *et al.* 2001). As a result, the growth rates of pro-HB-EGF, HB-EGF$_{\Delta N}$ and pSV-neo^r MLC were not significantly different from one another at 24, 48 or 72 h time points (Fig. 5c) suggesting that the amino- and carboxy-terminal domains of HB-EGF are mitogenic while membrane bound pro-HB-EGF is not mitogenic in MLCs.

Insulin-like activity by HB-EGF$_{\Delta N}$

Previous results in which HB-EGF was over-expressed in a transgenic mouse model identified kidney specific down-regulation of IGFBP-3 and -4 mRNA prior to the onset of puberty (Provenzano *et al.* 2005). Furthermore, we wished to determine whether the soluble, mature HB-EGF domain and/or HB-EGF C was responsible for the transcriptional regulation of IGFBPs using NRK cells transfected with pro-HB-EGF, HB-EGF$_{\Delta N}$ or mock transfected. Unlike MLCs, NRK cells exhibit detectable levels of IGFBP-3–5 and were used to characterize pro-HB-EGF and HB-EGF$_{\Delta N}$ responsiveness. NRK expression of pro-HB-EGF in NRK cells resulted in down-regulation of IGFBP-3 and -4 mRNA (Fig. 6, lanes 3 and 6) while HB-EGF$_{\Delta N}$ failed to down-regulate both IGFBP-3 and -4 mRNA (Fig. 6, lanes 4 and 7) as determined by semi-quantitative RT-PCR. IGFBP-5 was unaltered by either HB-EGF or HB-EGF$_{\Delta N}$ (Fig. 6, lanes 8–10). Non-transfected NRK cells exhibited similar levels of IGFBP-3, -4 and-5 mRNA as HB-EGF$_{\Delta N}$, suggesting that HB-EGF down-regulates IGFBP-3 and -4 mRNA rather than HB-EGF$_{\Delta N}$ up-regulating IGFBP-3 and -4 mRNA. GAPDH (Fig. 6, lanes 11–13) was used as an internal control to ensure that equivalent amounts of RNA were analysed.

DISCUSSION

Mammalian tissues often exhibit multiple isoforms of proteins that may result from post-translational processing and alternative splicing events. It has been previously reported that an alternatively spliced form of HB-EGF was cloned from a green monkey Vero cell cDNA library, termed the short form (SF) HB-EGF (Loukianov *et al.* 1997; Lukianov *et al.* 2002). This SF HB-EGF utilized an additional 94nt insert, exon 3a, between exon 3 and exon 4, which encoded the EGF domain of HB-EGF and caused a frameshift from codon 133 of pro-HB-EGF and premature termination (Lukianov *et al.* 2002). As a result, the mRNA encoded the signal peptide, pro-peptide, heparin-binding domain and a truncated EGF domain coding only the first two of three disulphide bonds that are all thought to be essential for binding to EGFRs with high affinity.

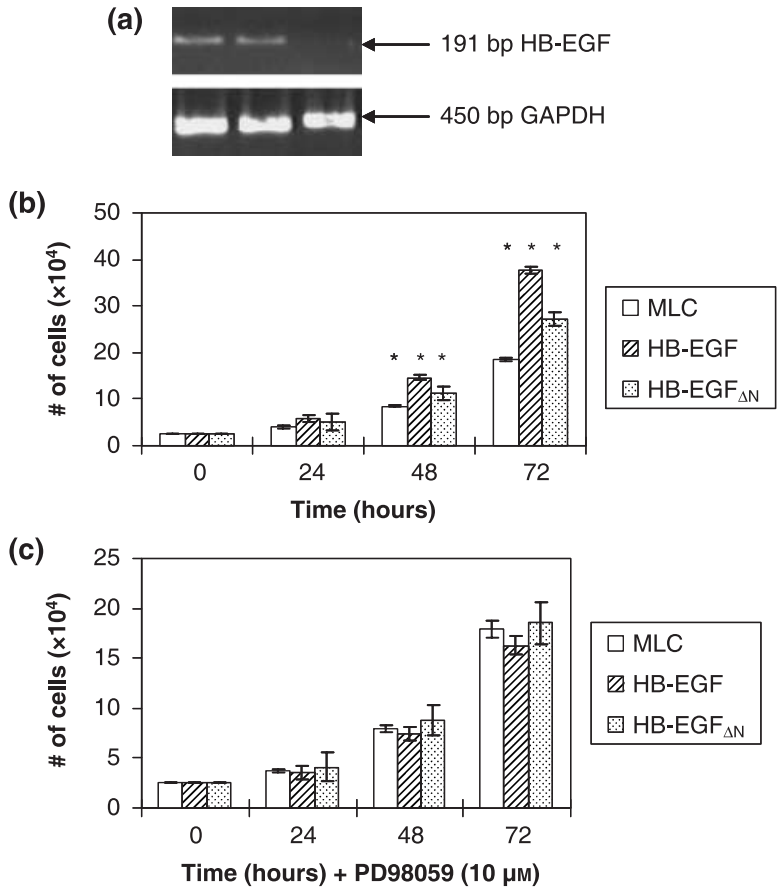

Figure 5. Induction of cellular proliferation by HB-EGF$_{\Delta N}$ and HB-EGF. (a) Semi-quantitative RT-PCR analysis of RNA from HB-EGF$_{\Delta N}$, HB-EGF and neo^r only stable cell lines using a primer set that amplifies the juxtamembrane, transmembrane and cytoplasmic domains of HB-EGF RNA (top panel, lanes 1–3, respectively). The expected 191-bp RT-PCR product is indicated in HB-EGF$_{\Delta N}$ and HB-EGF stable cell lines. A 450-bp GAPDH RT-PCR product is indicated to assure integrity of the RNA samples (bottom panel). (b) Cell population growth rates for 2×10^4 cells of HB-EGF$_{\Delta N}$, HB-EGF and neo^r stable cell lines examined over 72 h and (c) in the presence of 10 μM MAP kinase kinase inhibitor PD98059. The average number of cells ± SEM at 24, 48 and 72 h from two experiments performed in triplicate is indicated for each stable cell line. Data are representative of results collected from two independent HB-EGF and HB-EGF$_{\Delta N}$ stable cell lines each. Values of $P = 0.05$ were considered to be significant and indicated by an asterisk.

The product from this mRNA transcript demonstrated the ability to bind heparin with a high affinity, elutes from heparin-sepharose at high ionic strength (> 1.5 M NaCl), but bound EGFRs weakly, if at all (Lukianov *et al.* 2002). In this study, a human HB-EGF cDNA encoding only a portion of the amino-terminal EGF-like domain, including the third disulphide bond, juxtamembrane, transmembrane and cytoplasmic domains, termed HB-EGF$_{\Delta N}$, was characterized based on the presence of an amino-terminal truncated HB-EGF liver-specific transcript from mice. Unlike SF HB-EGF, the translational product of HB-EGF$_{\Delta N}$ is incapable of generating mature, soluble HB-EGF, which interacts with EGFRs upon ectodomain shedding, but does encode the carboxy-terminal HB-EGF C domain.

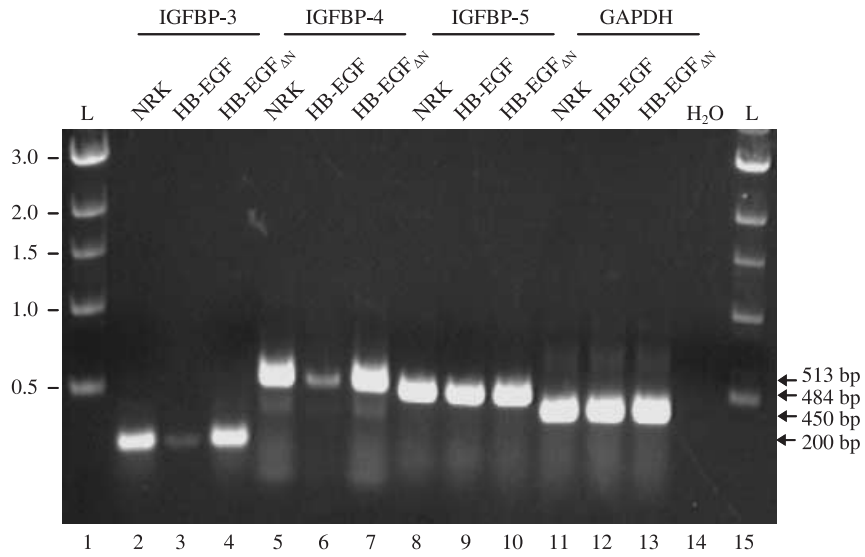

Figure 6. IGFBP-3, -4 and -5 mRNA analyses of NRK cells and NRK cells transfected with either HB-EGF or HB-EGF$_{\Delta N}$. Semi-quantitative RT-PCR with 1.0 μg of RNA from mock, HB-EGF and HB-EGF$_{\Delta N}$ transfected NRK cells using primers specific for IGFBP-3 (lanes 2–4), -4 (lanes 5–7), -5 (lanes 8–10) and GAPDH (lanes 11–13). Lane 14 is a control in which no RNA was added, but contains primer sets for all IGFBPs. A 1.0-kbp DNA ladder is shown in lanes 1 and 15.

Alternative splicing is an important cellular mechanism that leads to temporal and tissue-specific expression of unique mRNA products that encode various functional forms of a protein. The amino-terminal truncated, liver-specific, mouse HB-EGF mRNA transcript identified in this study may be a product of alternative splicing. Upon inspection of the previously published mouse HB-EGF DNA sequence (Harding *et al.* 1996), no consensus splice donor [C(or A)AG/GTA(or G)AGT] or acceptor splice sites [T(or C)$_n$NC(or T)AG/G], where $n = 12–14$ and N = pyrimidine, were observed between exons 1 and 4. However, RT-PCR results collected in this study demonstrate that a 255 nucleotide deletion within the extracellular-encoded region of the liver HB-EGF transcript occurred upstream of exon 4. One possibility may be that alternative splicing occurred from exon 1 to exon 4 resulting in the loss of 352 nucleotides. Further investigation, including cloning and sequencing of this unique HB-EGF transcript, is ongoing to characterize the possibility of alternative splicing. Nevertheless, identification of this transcript by RT-PCR served as a template to clone a human HB-EGF cDNA that lacks a functional EGF-like domain, yet encoding the juxtacrine, transmembrane and cytoplasmic domains of HB-EGF, termed HB-EGF$_{\Delta N}$.

It is clearly established that pro-HB-EGF undergoes proteolytic ectodomain shedding and is induced by treatment with the phorbol ester TPA (Goishi *et al.* 1995; Raab & Klagsbrun 1997) resulting in an amino-terminal mature, soluble domain of HB-EGF (12 kDa) capable of binding EGFRs. Subsequent and dependent on ectodomain shedding, is processing of the intracellular domain, through a yet unknown process, which yields a 6.5-kDa carboxy-terminal domain (HB-EGF C). HB-EGF C is phosphorylated at Ser$_{207}$ (Wang *et al.* 2006), translocates to the nucleus resulting in the nuclear export of the transcriptional repressor promyelocytic leukaemia zinc finger (PLZF) coordinating cell cycle progression (Nanba *et al.* 2003; Nanba & Higashiyama 2004; Toki *et al.* 2005). Generation of the HB-EGF-C occurs in response to pro-HB-EGF

ectodomain shedding because PLZF resides in the nucleus of HT1080 cells that stably express HB-EGF without treatment by TPA. However, the majority of PLZF is exported from the nucleus upon TPA treatment, suggesting that ectodomain shedding is necessary prior to the generation of HB-EGF C. Furthermore, two mutant HB-EGF knock-in mouse models have been characterized in which one expressed an uncleavable form of HB-EGF and the second expressed only the mature form of HB-EGF, lacking the transmembrane and cytoplasmic domains (HB-EGF$^{\Delta TM}$) (Yamazaki *et al.* 2003). Phenotypes of these mice displayed enlarged and dysfunctional hearts as well as malformed heart valves, which were similar to the phenotype exhibited by HB-EGF null mice (Jackson *et al.* 2003; Kiso *et al.* 2003; Yamazaki *et al.* 2003). Clearly, these results demonstrate the significance of HB-EGF ectodomain shedding for proper development.

Results from this study suggest that the entire amino-terminus of HB-EGF is not necessary for ectodomain shedding and amino acids 128–160 of pro-HB-EGF are sufficient for ectodomain cleavage followed by intracellular HB-EGF processing. The 8-kDa membrane-bound HB-EGF$_{\Delta N}$ translational product identified in this study undergoes proteolytic processing resulting in a 6.5-kDa HB-EGF C protein as demonstrated by HB-EGF Western blot analyses of stably transfected MLCs (Fig. 3, lane 2). Membrane preparations of HB-EGF$_{\Delta N}$ stably transfected MLCs identified both membrane-bound HB-EGF (8 kDa) and HB-EGF C (6.5 kDa) immunoreactive proteins, but only the 6.5-kDa HB-EGF C immunoreactive protein from cell extracts. This result may be attributed to residual proteolytic activity by ADAM during the membrane preparation.

A second indicator of pro-HB-EGF as well as HB-EGF$_{\Delta N}$ ectodomain shedding is tyrosine phosphorylation of MAP kinase kinase (pp42 kDa), an upstream event prior to and dependent on ectodomain shedding (Gechtman *et al.* 1999; Umata *et al.* 2001). We investigated the ability of both pro-HB-EGF and HB-EGF$_{\Delta N}$ expression in MLCs to induce tyrosine phosphorylation of a 42-kDa protein, because Western blot analyses indicate that both pro-HB-EGF and the amino-terminal truncated HB-EGF$_{\Delta N}$ undergo ectodomain shedding resulting in HB-EGF C (Fig. 3a). Consistent with previous results, pro-HB-EGF and HB-EGF$_{\Delta N}$ induce tyrosine phosphorylation of p42. The pp42 tyrosine-phosphorylated protein identified in this study is likely p42 extracellular signal-regulated kinase, as previously reported (Gechtman *et al.* 1999). We propose that the synthesis of the amino-terminal truncated liver specific HB-EGF transcript may be a novel transcriptional process to promote HB-EGF C production.

The levels of the ~0.8-kb HB-EGF mRNA transcript found in liver, encoding an HB-EGF C membrane-bound signalling molecule, and full-length 2.5-kb HB-EGF mRNA, encoding both soluble HB-EGF and HB-EGF C signalling molecules, were comparable suggesting that HB-EGF C may be important during development of mouse liver at 7 weeks of age, a time during or immediately after adolescence in mouse. *In vivo* data exist suggesting that HB-EGF is a potent hepatotrophic factor in transgenic mice in which the HB-EGF cDNA is specifically targeted to the liver resulting in accelerated proliferation of hepatocytes after partial hepatectomy (Kiso *et al.* 2003). The presence of both full-length and truncated HB-EGF transcripts, derived from the mouse HB-EGF gene, which yield mature soluble HB-EGF and HB-EGF C, respectively, suggests that dual signalling by HB-EGF (soluble, mature HB-EGF and HB-EGF C) may be important in liver function.

MLCs stably transfected with either HB-EGF$_{\Delta N}$ or HB-EGF stimulated cell division 1.3–2× greater than non-transfected MLCs, respectively. It is likely that, in addition to the generation of HB-EGF C, which is the only mitogenic domain formed from HB-EGF$_{\Delta N}$, the full-length HB-EGF transcript generates mature, soluble HB-EGF protein capable of interacting with EGFR on MLCs. This dual signalling by pro-HB-EGF results in significantly greater mitogenicity as compared to HB-EGF$_{\Delta N}$ and pSV-neo transfected MLCs. The observed difference between

HB-EGF$_{\Delta N}$ and pro-HB-EGF cell proliferation may be due to the presence of limited EGFRs on the MLCs that upon ectodomain shedding, soluble HB-EGF may bind and stimulate cell division (Harding *et al.* 1995). Hence, pro-HB-EGF MLCs stimulate cell division in both an EGFR-dependent and independent manner. The HB-EGF and HB-EGF$_{\Delta N}$, stable cell lines used in this study exhibited similar levels or expression as determined by semi-quantitative RT-PCR demonstrating that the differences in cell proliferation were not due to higher levels of protein of either pro-HB-EGF or HB-EGF$_{\Delta N}$ (Fig. 5a).

The EGF-like domain within HB-EGF, as well as within all EGF family members, encodes a conserved six cysteine motif ($CX_7CX_{4-5}CX_{10-13}CXCX_8C$) that contributes to the formation of three intramolecular disulphide bonds (C_1–C_3, C_2–C_4, C_5–C_6) that are presumed essential for HB-EGF mitogenicity (Carpenter *et al.* 1991; Higashiyama *et al.* 1991; Thompson *et al.* 1994). However, an alternatively spliced mRNA transcript of HB-EGF, HB-EGF SF, encodes a carboxy-terminal truncated EGF-like domain containing the first two disulphide bonds that weakly, if at all, bound EGFRs, but stimulated mitogenic activity (Luk'ianov *et al.* 2002). In contrast, HB-EGF$_{\Delta N}$ lacks the first two disulphide bonds within the EGF-like domain and stimulates cellular division via the carboxy-terminus of HB-EGF (HB-EGF C). These two lines of evidence clearly establish that a complete EGF-like domain containing three disulphide bonds is not necessary for the overall HB-EGF mitogenic activity, but may be critical in contributing to the structure of HB-EGF in order to bind EGFRs.

Taken together, our results suggests that upon analysis of mouse HB-EGF mRNA in kidney, lung and liver, the HB-EGF gene synthesizes the full-length 2.5-kb transcript in all tissues with the addition of a liver-specific amino-terminal truncated mRNA transcript that encodes the carboxy-terminal region of the EGF-like domain, including the third disulphide bond, juxtamembrane, transmembrane and cytoplasmic domains. Strikingly, both full-length and truncated HB-EGF mRNAs are present at similar levels in the liver of mice at 7 weeks of age, indicative of the importance of EGFR-dependent and independent signalling by HB-EGF in this tissue. As a result, the human HB-EGF$_{\Delta N}$ cDNA equivalent to this mouse transcript that lacks a functional EGF-like domain allows for identification of HB-EGF C specific cell signalling. We have recently demonstrated that over-expression of pro-HB-EGF in the kidney of transgenic mice down-regulates IGFBP-3 and -4 mRNA (Provenzano *et al.* 2005). However, because pro-HB-EGF generates both mature, soluble HB-EGF, as well as HB-EGF C upon processing, one cannot discern which HB-EGF domain is responsible for this phenomenon. Therefore, we demonstrate that the expression of HB-EGF$_{\Delta N}$ in IGFBP-responsive NRK cells, failed to down-regulated IGFBP-3 and -4 mRNA, whereas pro-HB-EGF expression down-regulated IGFBP-3 and -4 mRNA. These data suggest that HB-EGF regulates the insulin-like signalling pathway in NRK cells *via* soluble, mature HB-EGF interaction with EGFRs and not HB-EGF C. These data are consistent with studies in which administration of exogenous EGF reduced IGFBP-3 mRNA, suggesting that the insulin-like transcriptional regulation by EGF occurs by an EGFR-dependent pathway (Edmondson *et al.* 1999; Ozawa *et al.* 2004).

In this report, we have demonstrated the molecular cloning and expression of a human HB-EGF cDNA equivalent to the amino-terminal truncated HB-EGF transcript found in liver (HB-EGF$_{\Delta N}$), results in a membrane bound protein of 8 kDa that upon processing generates a 6.5-kDa cytoplasmic protein when expressed in MLCs. According to the model in which ectodomain shedding occurs prior to intracellular domain processing (Nanba *et al.* 2003), these results suggest that a 32-amino acid extracellular domain of HB-EGF$_{\Delta N}$ is sufficient for both ectodomain shedding followed by intracellular processing resulting in HB-EGF C. Furthermore, stable expression of HB-EGF$_{\Delta N}$ in MLCs induces tyrosine phosphorylation of pp42 and significantly stimulates cell proliferation when compared to non-transfected MLCs, but to a lesser

extent than MLCs that express the full-length HB-EGF cDNA. HB-EGF$_{\Delta N}$ lacked the ability to compete with ^{125}I-EGF in an EGFR binding assay, suggesting that HB-EGF$_{\Delta N}$ does not bind EGFRs. In conclusion, we present evidence of a novel mouse HB-EGF mRNA transcript specific to liver, in which a human HB-EGF cDNA equivalent to this transcript is expressed in MLC or NRK cells, stimulates mitogenic activity through an HB-EGF C signalling pathway independent of EGFRs and lacks the ability to down-regulate IGFBP-3 and -4 mRNA.

ACKNOWLEDGEMENTS

This research was supported by a Grant to Promote Research from the Miami University Committee on Faculty Research. The authors wish to thank Dr. Paul F. James, Dr. Jim Janik, and Dr. Lori Isaacson for helpful suggestions and review of the manuscript.

REFERENCES

Asakura M, Kitakaze M, Takashima S, Liao Y, Ishikura F, Yoshinaka T, Ohmoto H, Node K, Yoshino K, Ishiguro H, Asanuma H, Sanada S, Matsumura Y, Takeda H, Beppu S, Tada M, Hori M, Higashiyama S (2002) Cardiac hypertrophy is inhibited by antagonism of ADAM12 processing of HB-EGF; metalloproteinase inhibitors as a new therapy. *Nat. Med.* **8**, 35–40.

Besner G, Higashiyama S, Klagsbrun M (1990) Isolation and characterization of a macrophage-derived heparin-binding epidermal growth factor. *Cell Regul.* **1**, 811–819.

Carpenter G, Wahl MI (1991) The epidermal growth factor family. In: Sporn MB Roberts AB, eds. *Peptide Growth Factors and Their Receptors*, Vol. 1, p. 69–71. New York: Springer-Verlag.

Carraway KL 3rd, Weber JL, Unger MJ, Ledesma J, Yu N, Gassmann M, Lai C (1997) Neuregulin-2, a new ligand of ErbB3/ErbB4-receptor tyrosine kinases. *Nature* **387**, 512–516.

Chang H, Riese DJ 2nd, Gilbert W, Stern DF, McMahan UJ (1997) Ligands for ErbB-family receptors encoded by a neuregulin-like gene. *Nature* **387**, 509–512.

Derynck R, Roberts AB, Winkler ME, Chen EY, Goeddel DV (1984) Human transforming growth factor-alpha: precursor structure and expression in *E. coli*. *Cell* **38**, 287–297.

Edmondson SR, Murashita MM, Russo VC, Wraight CJ, Werther GA (1999) Expression of insulin-like growth factor binding protein-3 (IGFBP-3) in human keratinocytes is regulated by EGF and TGFβ. *J. Cell Physiol.* **179**, 201–207.

Gechtman Z, Alonso JL, Raab G, Ingber DE, Klagsbrun M (1999) The Shedding of Membrane Anchored Heparin-binding Epidermal-like Growth Factor Is Regulated by the Raf/Mitogen-activated Protein Kinase Cascade and by Cell Adhesion and Spreading. *J. Biol. Chem.* **274**, 28828–28835.

Goishi K, Higashiyama S, Klagsbrun M, Nakano N, Umata T, Ishikawa M, Mekada E, Taniguchi N (1995) Phorbol ester induces the rapid processing of cell surface heparin-binding EGF-like growth factor: conversion from juxtacrine to paracrine growth factor activity. *Mol. Biol. Cell* **6**, 967–980.

Harding PA, Brigstock DR, Shen L, Crissman-Combs MA, Besner GE (1996) Characterization of the gene encoding murine heparin-binding epidermal growth factor-like growth factor. *Gene* **169**, 291–292.

Harding PA, Davis-Fleischer KM, Crissman-Combs MA, Miller MT, Brigstock DR, Besner GE (1999) Induction of anchorage independent growth by heparin-binding EGF-like growth factor (HB-EGF). *Growth Factors* **17**, 49–61.

Harding PA, Wang XZ, Kopchick JJ (1995) Growth hormone (GH)-induced tyrosine phosphorylated proteins in cells that express GH receptors. *Receptor* **5**, 81–92.

Higashiyama S, Abraham JA, Miller J, Fiddes JC, Klagsbrun M (1991) A heparin-binding growth factor secreted by macrophage-like cells that is related to EGF. *Science* **251**, 936–939.

Higashiyama S, Iwamoto R, Goishi K, Raab G, Taniguchi N, Klagsbrun M, Mekada E (1995) The membrane protein CD9/DRAP27 potentiates the growth factor activity of the membrane-anchored heparin-binding EGF-like growth factor (HB-EGF). *J. Cell Biol.* **128**, 929–938.

Higashiyama S, Lau K, Besner GE, Abraham JA, Klagsbrun M (1992) Structure of heparin-binding EGF-like growth factor: multiple forms, primary structure and glycosylation of the mature protein. *J. Biol. Chem.* **267**, 6205–6212.

Hwa V, Oh Y, Rosenfeld RG (1999) The insulin-like growth factor-binding protein (IGFBP) superfamily. *Endocr. Rev.* **20**, 761–787.

Izumi Y, Hirata M, Hasuwa H, Iwamoto R, Umata T, Miyado K, Tamai Y, Kurisaki T, Sehara-Fujisawa A, Ohno S, Mekada E (1998) A metalloprotease-disintegrin, MDC9/meltrin-gamma/ADAM9 and PKCdelta are involved in TPA-induced ectodomain shedding of membrane-anchored heparin-binding EGF-like growth factor. *EMBO J.* **17**, 7260–7272.

Jackson LF, Qui TH, Sunnarborg SW, Chang A, Zhang C, Patterson C, Lee DC (2003) Defective valvulogenesis in HB-EGF and TACE-null mice is associated with aberrant BMP signaling. *EMBO J.* **22**, 2704–2716.

Jewell EA, Lingrel JB (1991) Comparison of the substrate dependence properties of the rat Na, K-ATPase alpha 1, alpha 2, and alpha 3 isoforms expressed in HeLa cells. *J. Biol. Chem.* **266**, 16925–16930.

Kiso S, Kawata S, Tamura S, Inui Y, Yoshida Y, Sawai Y, Umeki S, Ito N, Yamada A, Miyagawa J, Higashiyama S, Iwawaki T, Saito M, Taniguchi N, Matsuzawa Y, Kohno K (2003) Liver regeneration in heparin-binding EGF-like growth factor transgenic mice after partial hepatectomy. *Gastroenterology* **124**, 701–707.

Lemjabbar H, Basbaum C (2002) Platelet-activating factor receptor and ADAM10 mediate responses to Staphylococcus aureus in epithelial cells. *Nat. Med.* **8**, 41–46.

Loukianov E, Loukianova T, Wiedlocha A, Olsnes S (1997) Expression of mRNA for a short form of heparin-binding EGF-like growth factor. *Gene* **195**, 81–86.

Lukianov EV, Viedlokha A, Kuianskaia DV, Olsnes S, Kozlov IuV (2002) A short form of the heparin-binding EGF-like growth factor with a changed EGF domain. *Mol. Biol. (Mosk.)* **36**, 76–83.

Massague J, Pandiella A (1993) Membrane-anchored growth factors. *Annu. Rev. Biochem.* **625**, 15–41.

Nakagawa T, Higashiyama S, Mitamura T, Mekada E, Taniguchi N (1996) Amino-terminal processing of cell surface heparin-binding epidermal growth factor-like growth factor up-regulates its juxtacrine but not its paracrine growth factor activity. *J. Biol. Chem.* **271**, 30858–30863.

Nakamura Y, Handa K, Iwamoto R, Tsukamoto T, Takahasi M, Mekada E (2001) Immunohistochemical distribution of CD9, heparin binding epidermal growth factor-like growth factor, and integrin $\alpha 3\beta 1$ in normal human tissues. *J. Histochem. Cytochem.* **49**, 439–444.

Nanba D, Higashiyama S (2004) Dual intracellular signaling by proteolytic cleavage of membrane-anchored heparin-binding EGF-like growth factor. *Cytokine Growth Factor Rev.* **15**, 13–19.

Nanba D, Mammoto A, Hashimoto K, Higashiyama S (2003) Proteolytic release of the carboxy-termial fragment of proHB-EGF causes nuclear export of PLZF. *J. Cell Biol.* **163**, 489–502.

Nishi E, Klagsbrun M (2004) Heparin-binding epidermal growth factor-like growth factor (HB-EGF) is a mediator of multiple physiological and pathological pathways. *Growth Factors* **22**, 253–260.

Ozawa S, Kato Y, Shimuzu S, Suga M, Takamizawa S, Maehata Y, Okada S, Sato S, Kupota E, Hata R-I (2004) *Microarray Analysis of EGF-Regulated Gene Expression in Tongue Carcinoma Cells*. The IADR/AADR/CADR 82nd General Session (March 10–13, 2004), #3708.

Plowman GD, Culouscou JM, Whitney GS, Green JM, Carlton GW, Foy L, Neubauer MG, Shoyab M (1993) Ligand-specific activation of HER4/p180erbB4, a fourth member of the epidermal growth factor receptor family. *Proc. Natl. Acad. Sci. USA* **90**, 1746–1750.

Plowman GD, Green JM, McDonald VL, Neubauer MG, Disteche CM, Todaro GJ, Shoyab M (1990) The amphiregulin gene encodes a novel epidermal growth factor-related protein with tumour-inhibitory activity. *Mol. Cell. Biol.* **5**, 1969–1981.

Provenzano AP, Besner GE, James PF, Harding PA (2005) Heparin-binding EGF-like growth factor (HB-EGF) over-expression in transgenic mice downregulates insulin-like growth factor binding protein (IGFBP) -3 and -4 mRNA. *Growth Factors* **23**, 19–31.

Raab G, Klagsbrun M (1997) Heparin-binding EGF-like growth factor. *Biochim. Biophys. Acta* **1333**, 179–199.

Rajaram S, Baylink DJ, Mohan S (1997) Insulin-like growth factor-binding proteins in serum and other biological fluids: regulation and functions. *Endocr. Rev.* **18**, 801–831.

Shing Y, Christofori G, Hanahan D, Ono Y, Sasada R, Igarashi K, Folkman J (1997) Betacellulin: a mitogen from pancreatic beta cell tumors. *Science* **259**, 1604–1607.

Stroobant P, Rice AP, Gullick WJ, Cheng DJ, Kerr IM, Waterfield MD (1985) Purification and characterization of vaccinia virus growth factor. *Cell* **42**, 383–393.

Sunnarborg SW, Hinkle CL, Stevenson M, Russell WE, Raska CS, Peschon JJ, Castner BJ, Gerhart MJ, Paxton RJ, Black RA, Lee DC (2002) Tumor necrosis factor-alpha converting enzyme (TACE) regulates epidermal growth factor receptor ligand availability. *J. Biol. Chem.* **277**, 12 838–12 845.

Thompson SA, Higashiyama S, Wood K, Pollitt NS, Damm D, McEnroe G, Garrick B, Ashton N, Lau K, Hancock N, Klagsbrun M, Abraham J (1994) Characterization of sequences within heparin-binding EGF-like growth factor that mediate interaction with heparin. *J. Biol. Chem.* **269**, 2541–2549.

Toki F, Nanba D, Matsuura N, Higashiyama S (2005) Ectodomain shedding of membrane-anchored heparin-binding EGF like growth factor and subcellular localization of the C-terminal fragment in the cell cycle. *J. Cell Physiol.* **202**, 839–848.

Toyoda H, Komurasaki T, Uchida D, Takayama Y, Isobe T, Okuyama T, Hanada K (1995) Epiregulin. A novel epidermal growth factor with mitogenic activity for rat primary hepatocytes. *J. Biol. Chem.* **270**, 7495–7500.

Umata T, Hirata M, Takahashi T, Ryu F, Shida S, Takahashi Y, Tsuneoka M, Miura Y, Masuda M, Horiguchi Y, Mekada E (2001) A dual signaling cascade that regulates the ectodomain shedding of heparin-binding epidermal growth factor-like growth factor. *J. Biol. Chem.* **276**, 30 475–30 482.

Wang X, Minzushima H, Adachi S, Shishi M, Iwamoto R, Mekada E (2006) Cytoplasmic domain phosphorylation of heparin-binding EGF-like growth factor. *Cell Struct. Funct.* **31**, 15–27.

Yamazaki S, Iwamoto R, Saeki K, Asakura M, Takashima S, Yamazaki A, Kimura R, Mizushima H, Moribe H, Higashiyama S, Endoh M, Kaneda Y, Takagi S, Itami S, Takeda N, Yamada G, Mekada E (2003) Mice with defects in HB-EGF ectodomain shedding show severe developmental abnormalities. *J. Cell Biol.* **163**, 469–475.

Yan Y, Shirakabe K, Werb Z (2002) The metalloprotease Kuzbanian (ADAM10) mediates the transactivation of EGF receptor by G protein-coupled receptors. *J. Cell Biol.* **158**, 221–226.